Article

Preparation and Evaluation of Vancomycin-Loaded *N*-trimethyl Chitosan Nanoparticles

Jiaojiao Xu [1,2,†]**, Beihua Xu** [2,†]**, Dan Shou** [3]**, Xiaojing Xia** [2] **and Ying Hu** [1,2,*]

[1] Department of Medicine, Wenzhou Medical University, Wenzhou 325000, China;
  E-Mail: xjj_1204@yeah.net

[2] Zhejiang Pharmaceutical College, Ningbo 315000, China; E-Mails: xvbeihua@163.com (B.X.);
  maysummer@163.com (X.X.)

[3] Department of Medicine, Zhejiang Academy of Traditional Chinese Medicine, Hangzhou 310000,
  China; E-Mail: shoudanok@163.com

[†] These authors contributed equally to this work.

[*] Author to whom correspondence should be addressed; E-Mail: pharmhawk@126.com;
  Tel.: +86-574-8822-2707; Fax: +86-574-8822-3023.

Academic Editor: Jianxun Ding

Abstract: Chronic intracellular infections caused by drug-resistant pathogens pose a challenge to the treatment of chronic osteomyelitis. Such treatment requires an intracellular delivery system for the sustained release of antibiotics such as vancomycin (VCM), which is an antibiotic of last resort used against many clinically resistant bacteria. In this work, we report VCM-loaded *N*-trimethyl chitosan (TMC) nanoparticles and their potential application for drug delivery. The results showed that the prepared nanoparticles were predominantly spherical in shape with an average particle diameter of 220 nm, a positive zeta potential, and a loading efficiency of 73.65% $\pm$ 1.83%. Furthermore, their drug release profile followed the Higuchi model for sustained release, with non-Fickian diffusion. Over a 24-h period, 6.51% $\pm$ 0.58% of the drug within the optimized nanoparticles was released. *In vitro* cytology showed that osteoblasts (OBs) exhibited higher alkaline phosphatase activity (ALP) after exposure to TMC nanoparticle material. Furthermore, TMC nanoparticles increased the uptake of water-soluble quantum dots (QDs) by OBs, and both nanoparticles and VCM/TMC mixtures improved OB proliferative activity. We also investigated the minimum inhibitory concentration (MIC, 60 µg/mL), half maximal inhibitory concentration (IC50, 48.47 µg/mL), diameter of inhibition zone (DIZ, 1.050 cm),

and turbidimetric (TB) assay of nanoparticles. All data demonstrated that VCM/TMC nanoparticles had excellent antibacterial activity against the Gram-positive bacterium *Staphylococcus aureus*. These findings suggest that VCM-loaded TMC nanoparticles have good potential for the sustained delivery of antibiotics to bone infections.

Keywords: vancomycin (VCM); *N*-trimethyl chitosan (TMC); intracellular infections; nanoparticles

1. Introduction

Chronic osteomyelitis, an osseous infection, causes severe recurrent inflammation, hastens the presence of necrotic bone and sequestrum, and can lead to other serious complications if left untreated. It is commonly caused by pathogenic microorganisms, which can adhere to and even invade mammalian cells. However, drug-resistant pathogens such as methicillin-resistant *Staphylococcus aureus* (MRSA) and multidrug-resistant (MDR) mycobacteria, have developed the ability to persist in intracellular locations.[1] Many antibiotic families are hydrophilic or exhibit low intracellular retention, which hinders their effectiveness because they are unable to penetrate cells.[2] Furthermore, chronic osteomyelitis is intrinsically resistant to antibiotic treatment, even when caused by bacteria that are not among the drug-resistant strains, mainly because they frequently form biofilms on necrotic bone and foreign bodies, making them up to 800-fold less susceptible to antibiotics than planktonic forms [3].

Glycopeptide antibiotics, such as vancomycin (VCM), a tricyclic glycosylated nonribosomal peptide, act against Gram-positive bacteria. This family of antibiotics is used as a last resort for the treatment of drug-resistant bacteria. VCM acts by inhibiting cell wall synthesis in Gram-positive bacteria, and prevents cross-linking between any cell wall polymers that do manage to form.

Instead of looking for new antibiotics, research on the treatment of chronic osteomyelitis has turned toward new delivery systems. Nanocarriers [1,4,5], such as liposomes and nanoparticles, offer high intracellular penetration and the potential for effective intracellular antibacterial activity over extended time periods. Zakeri-Milani *et al.* improved the intestinal permeation of VCM by using VCM-loaded poly(lactide-*co*-glycolide) (PLGA) nanoparticles [6]. VCM solid lipid nanoparticles, adjuvanted with linoleic acid, exhibited higher antibacterial activity than VCM towards both susceptible and resistant bacteria [7]. The biggest limitations associated with most nanocarriers are poor release profiles, with some having an initial burst phase in which most of the drug is lost, or weak antibacterial activities that require the use of very high antibiotic concentrations. Until now, no studies have been published on the application of VCM-loaded *N*-trimethyl chitosan (TMC) nanoparticles for intracellular infections, or on detailed evaluations of the properties of the TMC polymer nanoparticle material, which could overcome limitations associated with other materials.

In the present study, with the aim to increase the sustained effectiveness of intracellular antibiotics, VCM-loaded TMC nanoparticles were prepared by single ionic complexation. Dynamic light scattering (DLS), transmission electron microscopy (TEM), and atomic force microscopy (AFM) were performed to characterize the test formulations. Dialysis was performed to evaluate the drug release, which was measured by reverse-phase high performance liquid chromatography (HPLC). *In vitro* cytology

examining alkaline phosphatase (ALP) activity, cell uptake ability, proliferative ability, and the effect on antibacterial activity, including minimum inhibitory concentration (MIC), half maximal inhibitory concentration (IC50), diameter of inhibition zone (DIZ), and turbidimetric (TB) assay were also analyzed for the nanoparticles (Scheme 1).
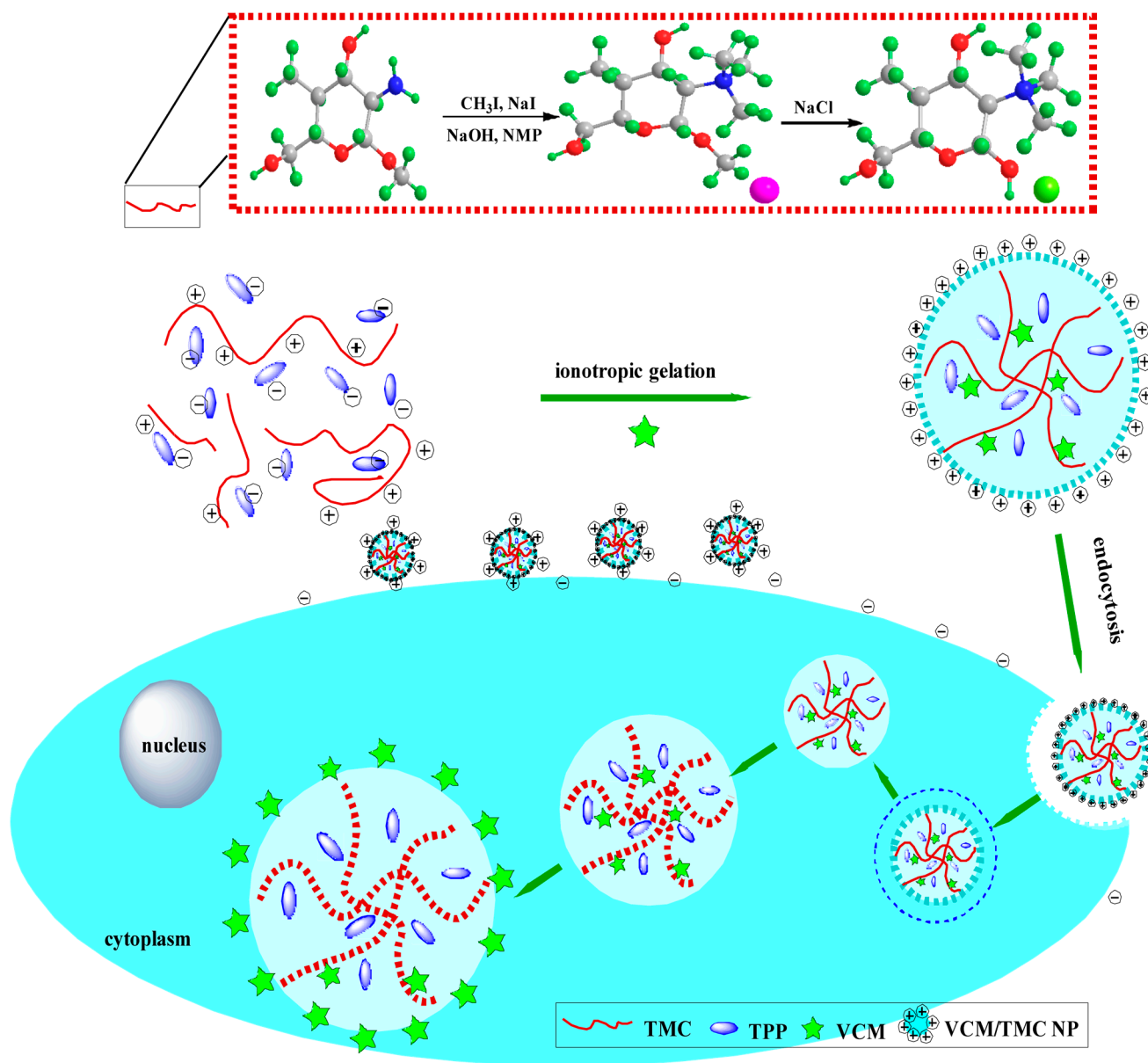
Scheme 1. A schematic diagram showing the formation of TMC polymer and VCM-loaded TMC nanoparticles, and the interaction between nanoparticles and cells during the uptake process. NMP, *N*-methylpyrrolidone; TMC, *N*-trimethyl chitosan; TPP, sodium tripolyphosphate; VCM, vancomycin; NP, nanoparticle.

2. Experimental Section

2.1. Materials

Vancomycin hydrochloride (VCM-HCl) was supplied by Dalian Meilun Biotech Co., Ltd. (Dalian, China). Chitosan (600 K) was obtained from Zhejiang Golden-Shell Biochemical Co., Ltd.

(Zhejiang, China). *N*-(2-hydroxyethyl) piperazine-*N'*-(2-ethanesulphonic acid) (Hepes) and sodium tripolyphosphate (TPP) were purchased from Aladdin (Shanghai, China). *N*-methylpyrrolidone (NMP), sodium iodide, and iodomethane were purchased from Shanghai Sinopharm Chemical Reagent Company (Shanghai, China). Spectra/Por dialysis tubing (MWCO 2 kDa) (Spectrum Labs, Inc., New York, NY, USA) was used as received. Beyotime Institute of Biotechnology (Zhejiang, China) supplied the Cytotoxicity Assay Kit and all cell culture reagents. Carboxy-CdSe/ZnS quantum dots (QDs, water-soluble red fluorescent) were purchased from Beijing Zhongke Wu Yuan Biotechnology Co., Ltd. (Beijing, China). Methanol (HPLC grade) was purchased from Fisher Chemical (Suzhou, China). Other reagents and chemicals were of analytical reagent grade, unless indicated otherwise.

2.2. High-Performance Liquid Chromatography Analysis

Reverse-phase high performance liquid chromatography (HPLC, UltiMate3000, Dionex, Sunnyvale, CA, USA) was used to determine the antibiotic concentration of VCM. Briefly, chromatography was performed on a C18 analytical column (Agilent, Foster City, CA, USA, 4.6 mm × 250 mm) at 37 °C, with a flow rate of 0.7 mL/min. The mobile phase consisted of methanol and potassium dihydrogen phosphate buffer (0.025 mol/L, pH 3.2) mixed at a ratio of 20:80 (*v/v*). The peaks were identified via UV absorbance at 230 nm and the injection volume was 20 μL. The calibration curves exhibited linear behavior ($R^2 = 0.9998$) over the concentration range of 5–100 μg/mL, and were fit to the linear equation of $A = 0.7948C + 0.0761$.

2.3. Synthesis and Characterization of N-Trimethyl Chitosan (TMC)

A mixture of chitosan (2 g) and NMP (80 mL) were stirred at room temperature overnight. Sodium iodide (4.8 g) and 15% NaOH solution (11 mL) were added and stirred at 60 °C for 20 min, following which iodomethane (12 mL) was added. After 2 h of reaction, 15% NaOH solution (11 mL) and iodomethane (6 mL) were added to the reaction mixture. The reaction was continued for 2 h. The reaction mixture was then cooled and poured into ethanol (600 mL). The precipitate was filtered and dissolved in 10% NaCl solution (30 mL), which was then poured into ethanol (150 mL). The precipitate was filtered and dissolved in ultrapure water (16 mL), and subsequently dialyzed with deionized water for two days and lyophilized. The purified TMC was analyzed by Fourier transform infrared spectroscopy (FT-IR, Spectrum One, PerkinElmer, Foster City, CA, USA), with the sample embedded in KBr pellets, and proton nuclear magnetic resonance spectroscopy (^{1}H NMR, DMX-400, Bruker, Rheinstetten, Germany) with the sample dissolved in D_2O.

2.4. Preparation of TMC Nanoparticles

Simple ionic complexation was used to prepare both plain TMC nanoparticles and VCM-loaded TMC nanoparticles. For a 10 mL batch of nanoparticles, a TPP solution (1 mg/mL, serving as a physical crosslinker) was added to a solution of TMC (1 mg/mL, dissolved in Hepes pH 7.4) at a drop rate of 6 mL/h, under continuous stirring (200 rpm), to a final TMC:TPP weight ratio of 10:1.8. At this point, the solution became opalescent and uniform in appearance. After 1.5 h of stirring, the nanoparticle suspension was collected by centrifugation (10 min, 12,000 g) and re-suspended in water. VCM-loaded

TMC nanoparticles were prepared in the same way as non-loaded TMC nanoparticles, by co-dissolving the antibiotic (1 mg) in the TMC solution. Solid preparations of nanoparticle powder were prepared by freeze-drying the nanoparticle solutions.

2.5. Characterization of VCM/TMC Nanoparticles

2.5.1. Particle Size and Zeta Potential

Particle size, size distribution and zeta potential of the prepared nanoparticles were measured on a Malvern Zetasizer Nano ZS90 (Malvern Instruments Ltd., Malvern, UK). The particle size distribution was reported as the polydispersity index (PDI).

2.5.2. Nanoparticle Visualization

The morphology of the nanoparticles was observed via TEM (JEOL2010F, Jeol, Tokyo, Japan). TEM samples were prepared by placing a drop of nanoparticle suspension onto a 200-mesh carbon-coated copper grid. The excess aqueous solution was removed by blotting with filter paper after 2 min. Nanoparticles were also visualized with AFM (Dimension 3100 V, Veeco Instruments Inc., New York, NY, USA) in contact mode, where the samples were prepared by depositing a drop of the VCM/TMC nanoparticle solution onto a glass slide and allowing it to dry.

2.6. Drug Loading

The drug loading and loading efficiency of the VCM/TMC nanoparticles was determined as follows: 400 μL of VCM/TMC nanoparticle suspension were placed in an Amicon Ultra 10K centrifugal filter (Millipore, Eschborn, Germany), and subjected to centrifugation at 10,000g for 10 min at room temperature. The filtrate was collected and injected into the HPLC apparatus, and the VCM content was quantified by comparison to a standard curve. Each batch of samples was measured in triplicate. The loading efficiency and the drug loading were calculated according to Equations (1) and (2), respectively, as follows:

$$\text{Loading efficiency} (\%, w/w) = (\text{Total amount of drug} - \text{Free drug})/\text{Total amount of drug} \quad (1)$$

$$\text{Drug loading} (\%, w/w) = (\text{Mass of drug in nanoparticles})/(\text{Mass of nanoparticles}) \quad (2)$$

2.7. In Vitro Stability of TMC Nanoparticles

To measure the colloidal stability of the nanoparticles, the nanoparticle suspension was diluted in 5 mM Hepes (pH 7.4) to obtain the appropriate TMC concentration. The nanoparticles were stored at 37 °C and their size and PDI were measured after 1, 2, 4, 10, 24 and 48 h.

2.8. In Vitro Drug Release Study and Kinetic Modeling

The release of drug from the nanoparticles was measured in PBS (pH 7.4), using equilibrium dialysis. 1 milliliter of VCM/TMC nanoparticle dispersion was placed in cylindrical tubing and suspended in 4 mL of PBS (pH 7.4) in a flotation dialysis device (5 mL, 2 kDa MWCO, Sangon Biotech Co., Ltd, Shanghai, China). The temperature of the system was maintained at 37 ± 2 °C with a rotation speed of 100 rpm (Thermostatic water bath oscillators, Jiangsu Huanyu Scientific Institute, WHY-2, JiangSu, China). 400 microliter of the buffer solution was sampled periodically at predetermined intervals and was replaced with the same volume of fresh PBS (pH 7.4). The amount of released drug was then determined by HPLC and calculated as cumulative percent release. Sink conditions were maintained for the release study and the experiments were performed in triplicate.

To propose a release mechanism, the data obtained from *in vitro* drug release studies were plotted and fitted to the following kinetic models: zero order, first order, Higuchi, and Hixson-Crowell. The best fit was evaluated by calculating the correlation coefficient. Additionally, to understand the release mechanism, the release data were fitted to the Korsmeyer–Peppas model ($M_t/M_\infty = Kt_n$), where, M_t/M_∞ is fraction of drug released at time t, K is the rate constant and the exponent "n" represents the drug transport mechanism and can be used to evaluate the mechanism of diffusion [8].

2.9. In Vitro Cellular Study

2.9.1. Cell Line and Culture Media

A mouse osteoblast (OB) cell line was obtained as a gift from the Experimental Animal Center of Zhejiang University (Zhejiang, China) and used as received. Cells were cultured in Dulbecco's Modified Eagle's Medium (DMEM, GIBCO, New York, NY, USA), supplemented with 10% (*v/v*) heat-inactivated fetal bovine serum (FBS), 100 units/mL penicillin and 100 units/mL streptomycin, and incubated in 5% CO_2 at 37 °C and 95% relative humidity.

2.9.2. Alkaline Phosphatase Activity

Alkaline phosphatase (ALP) activity was measured to assess cell differentiation using an Alkaline Phosphatase Assay Kit (Nanjing Jiancheng Bioengineering Institute, Nanjing, China) and BCA (bicinchoninic acid) Protein Assay Kit (Beyotime Institute of Biotechnology, Shanghai, China), according to the manufacturers' specifications. In brief, OBs were placed in a 24-well plate at a seeding density of (4.0×10^4)–(5.0×10^4) per well. After incubation overnight, cells were exposed to 1 mg/mL plain TMC nanoparticles (TMC-TPP) or β-tricalcium phosphate (β-TCP) suspension (dissolved in sterilized water) and incubated for four or seven days. The osteogenic medium was changed once every three days. At pre-determined time intervals, cell lysates were obtained by removing the medium, washing the cells with PBS (pH 7.4), and incubating cells with 1% Triton X-100 for 1.5 h. Each determination was standardized with respect to total protein, which was measured by BCA protein assay.

2.9.3. Cell Uptake Study

Water-soluble red fluorescent QDs were used as a model drug and the QDs/TMC-TPP nanocomplexes were formed as described previously, and its cellular uptake was compared with free QDs that were dissolved in PBS (pH 7.4). OBs were seeded in a six-well plate at a density of 5×10^5 cells/well. After incubating and reaching 70%–80% confluency, the cells were washed three times with PBS (pH 7.4), and then exposed for 4 h in the dark at 37 °C to FBS-free DMEM (650 μL) containing 100 μL of QDs/TMC-TPP nanocomplexes or free QDs. Non-drug-treated groups were used as controls. Following treatment, the cells were washed twice with PBS (pH 7.4), detached with trypsin, resuspended in DMEM with FBS, and immediately collected for analysis via flow cytometry (BD Biosciences, San Jose, CA, USA). For each sample, 10,000 events were recorded in the flow cytometer. All samples were measured in triplicate.

2.9.4. Cell Proliferation

The influence of VCM/TMC nanoparticles on the proliferation of OBs was evaluated *in vitro* by MTT (3-(4,5-dimethylthiazol-2-yl)-2,5-diphenyltetrazolium bromide) assay. This assay was also performed on VCM/TMC solution and VCM solution, where both solutes were dissolved in sterilized water. Briefly, exponentially growing cells were seeded in a 96-well plate at a seeding density of (4.0×10^3)–(5.0×10^3) cells per well, and cultured for 24 h. The cells were treated with various samples containing the same drug concentration of 0.1 mg/mL. Control wells were treated with equivalent volumes of drug-free medium. After 10 h, 10 μL MTT (5 mg/mL, dissolved in MTT assay solvent) was added to each well and the cells were further incubated for 4 h. After incubation, 100 μL of formazan dissolution buffer was added to each well to dissolve the MTT formazan crystals. The plates were shaken for 5 min and their absorbance was measured at 570 nm using a microplate reader. The experiments were repeated five times, and the results were expressed as a percentage viability of the control cells.

2.10. Ex Vivo Antibacterial Analysis

2.10.1. Bacterial Culture

The bacterial strain used in this study was the Gram-positive *Staphylococcus aureus* (*S. aureus*, ATCC 6538), which was purchased from Shanghai BioRc Co., Ltd. (Shanghai, China). *S. aureus* was cultured in LB (lysogeny broth 10 g of tryptone, 5 g of yeast extract and 10 g of NaCl per liter) on a shaker at 37 °C overnight until the optical density (OD) at 600 nm reached 0.5, indicating that the bacterial content reached approximately 10^8 colony forming units (CFU)/mL. For preparing the solid plate, an additional 25 g of agar per liter was added to LB liquid medium and all of the test bacterial groups were incubated in biochemical incubator (SHP-250, Shanghai Senxin Science Instrument Co., Ltd., Shanghai, China) with an atmosphere of 5% carbon dioxide at 37 °C.

2.10.2. Minimum Inhibitory Concentration Test

The LB broth microdilution method was used to determine the lowest concentration of VCM/TMC nanoparticles that can inhibit the growth of *S. aureus*, and two control groups were maintained for each test batch, including an antibiotic control (containing drugs and LB broth without inoculum) and a bacterial control (containing the LB broth and inoculum). 2 milliliter of prepared VCM/TMC nanoparticles and VCM solution, at concentrations of 6.25, 12.5, 25, 50, 60, 70, 80 and 90 μg/mL, were added to the test tubes with 100 μL bacterial suspension (containing approximately 1×10^6 CFU/mL). After culturing at 37 °C for 24 h, the turbidity was visually assessed by eye and a UV-VIS spectrometer at 600 nm, and the MIC values were interpreted as the point at which there was no development of turbidity. All samples were examined in triplicate.

2.10.3. Half Maximal Inhibitory Concentration (IC50) Test

The half maximal inhibitory concentration (IC50) of the VCM/TMC nanoparticles was determined via a solid culture CFU assay, in which a plate without nanoparticles was used as negative control. Briefly, a 100-μL aliquot of the standardized inoculum (2×10^6 CFU/mL) was mixed with 2 mL of a series of concentrations of VCM/TMC nanoparticles or VCM solution (6.25, 12.5, 25, 30, 40, 50, 60, 70, 80 and 90 μg/mL), incubated for 24 h at 37 °C, and then 25 μL of the prepared mixtures were spread on LB solid sugar plates. By calculating and comparing the reliable value of CFU with the control, we determined the IC50 values for each sample. Each assay was repeated in triplicate.

2.10.4. The Diameter of Inhibition Zone Test

To ensure the susceptibility of *S. aureus* to VCM/TMC nanoparticles, we measured zones of growth inhibition by the agar disk diffusion assay. Briefly, sterile filter discs (6 mm in diameter) were impregnated with 100 μL of VCM/TMC nanoparticle solution (50, 60, 70 and 80 μg/mL), VCM solution (50, 60, 70 and 80 μg/mL) or PBS (pH 7.4) control solution for about 30 min, and then plated on the surface of LB agar plates, in which approximately 10^6 CFU of *S. aureus* were previously inoculated (each plate contained four paper discs). After incubation for 24 h at 37 °C, the DIZ, in which there was no visible bacterial growth, was determined as an average of four measurements, in four perpendicular directions, using a vernier caliper. All tests were performed in triplicate.

2.10.5. Turbidimetric Assay

The TB assay was used to determine the antibacterial effects of VCM/TMC nanoparticles against the growth and proliferation of *S. aureus*. LB broth alone was used as a blank and samples without drug were used as the control group. As mentioned above, 200 μL of the bacteria, at a density of (4.0×10^5)–(5.0×10^5) CFU/mL, were mixed with 20 μL of nanoparticles or VCM solution at concentrations of 6.25, 12.5, 25, 30, 40, 50, 60, 70, 80 and 90 μg/mL, and placed in 96 well plates. After culturing for 24 h, a microplate reader (XMARK, Bio-Rad, Hercules, CA, USA) was used to measure the OD at 600 nm and the results were described as a percentage of bacterial viability, which was calculated as follows:

$$\text{Bacteria viability} = (\text{OD}_\text{test} - \text{OD}_\text{blank})/(\text{OD}_\text{control} - \text{OD}_\text{blank}) \times 100\% \tag{3}$$

Each concentration was repeated four times.

2.11. Statistical Analysis

Statistical analysis was performed using the software program GraphPad Prism 5 (GraphPad Software Inc., La Jolla, CA, USA). Data are presented as mean $\pm$ standard deviation (SD) for all results. Statistical significance was determined either by a paired *t* test or a one-way analysis of variance (ANOVA) with Bonferroni's or Dunnett's *post hoc* tests, depending on the experimental setup. A value of $p < 0.05$ (two-tailed) was considered to be statistically significant.

3. Results and Discussion

3.1. Synthesis and Characterization of TMC

N-trimethyl chitosan (TMC) was synthesized according to the mechanism shown in Figure 1. Characteristic structural changes attributed to TMC were confirmed by Fourier transform infrared (FTIR) spectroscopy. In comparison with the infrared (IR) spectrum of chitosan (CS, Figure 2A), a new band at 1475 cm^{-1}, attributed to asymmetrical stretching of C–H in the methyl groups on the quaternary ammonium, appeared in the spectrum of TMC (Figure 2B). The band at 1599 cm^{-1}, assigned to angular deformation of N–H in the amino groups on CS, was not observed in the spectrum of TMC, indicating that the CS amino groups were methylated.
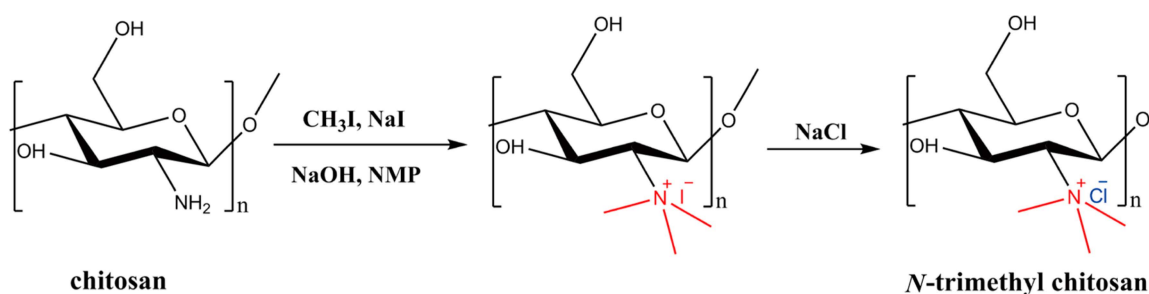
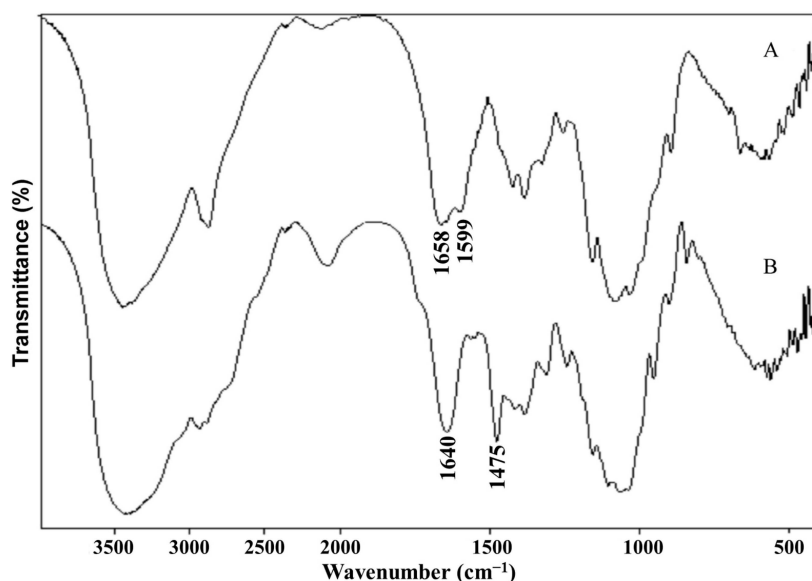**Figure 1.** The synthesis of *N*-trimethyl chitosan (TMC).

Figure 2. IR spectra of samples prepared in KBr pellets. (**A**) Chitosan (CS) and (**B**) *N*-trimethyl chitosan (TMC).

The proton nuclear magnetic resonance (^{1}H-NMR) spectrum of TMC is shown in Figure 3. According to the literature [9,10], the signal at 3.22 ppm corresponds to the methyl group at the *N,N,N*-trimethylated site, the signal at 2.72 ppm corresponds to the methyl group at the *N,N*-dimethylated site, and the signals ranging from 4.8 to 5.4 ppm are attributed to the hydrogen atom bonded to the carbon 1 of the glycoside ring.
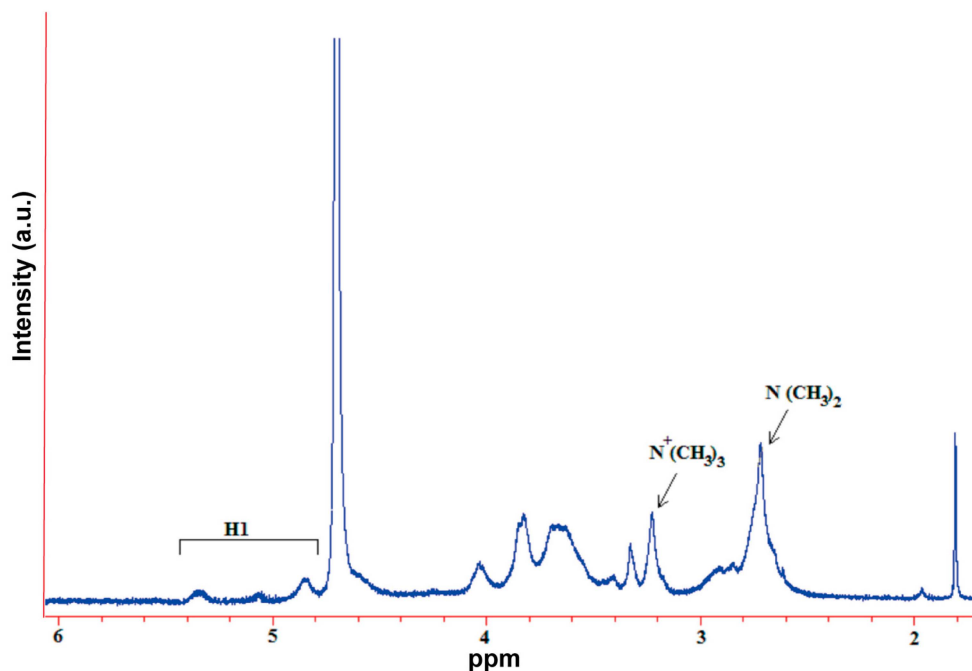

Figure 3. Characteristic ^{1}H-NMR spectrum of *N*-trimethyl chitosan (TMC) in D_2O.

The average degree of quaternization (DQ) of TMC was obtained using Equation (4), which compares the area of the peak corresponding with the methyl hydrogens of the trimethylated amino group (ATM) with the area of the peak corresponding to the hydrogen atoms bonded to carbon 1 (AH1). Thus, the DQ of TMC in this study was calculated as approximately 20%.

$$DQ\% \ = \ ((ATM/AH1) \times 1/9) \times 100 \tag{4}$$

3.2. Characterization of VCM/TMC Nanoparticles

Nanoparticles were prepared from the synthesized TMC having a DQ of 20%, which is in the range that was nontoxic according to previous studies [11,12]. We used ionotropic gelation to successfully prepare VCM/TMC nanoparticles. This technique relies on the interaction between negatively charged polyanions and positively charged TMC to form covalently crosslinked networks. In this study, all VCM-loaded nanoparticles showed a mean size distribution between 220 and 230 nm with a fairly monodisperse polydispersity index, which is almost below 0.2 (Figure 4A). The size of the particles could be varied by changing the amount of TPP that was added, over a very small range (200–325 nm), which is consistent with previous studies. Twelve TMC nanoparticles carried a positive zeta potential of 14.6 ± 0.8 mV at physiological pH (Figure 4B). TEM images (Figure 5A) indicate that the nanoparticles were spherical in shape, with no obvious particle aggregation; this was further confirmed by AFM

(Figure 5B), and is not consistent with the previous finding that nanoparticles loaded with antigen have an irregular shape [13].
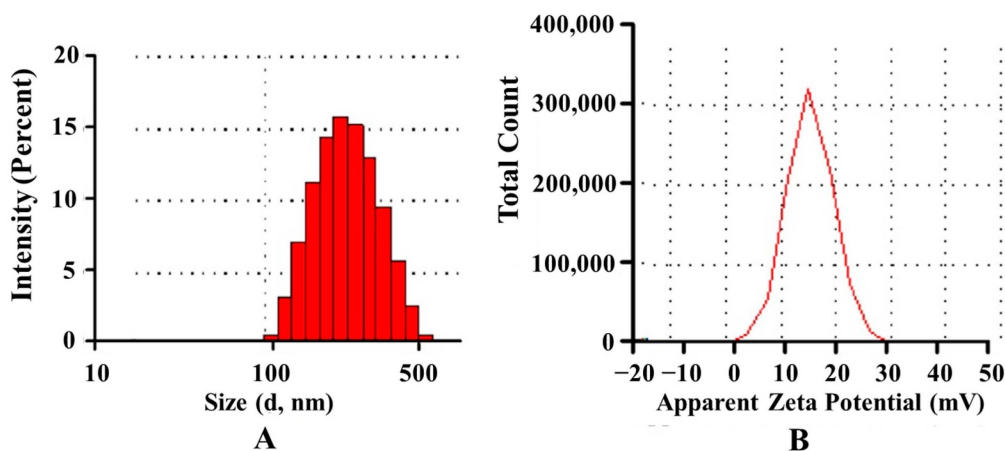

Figure 4. (**A**) Size distribution and (**B**) zeta potential of VCM/TMC nanoparticles.
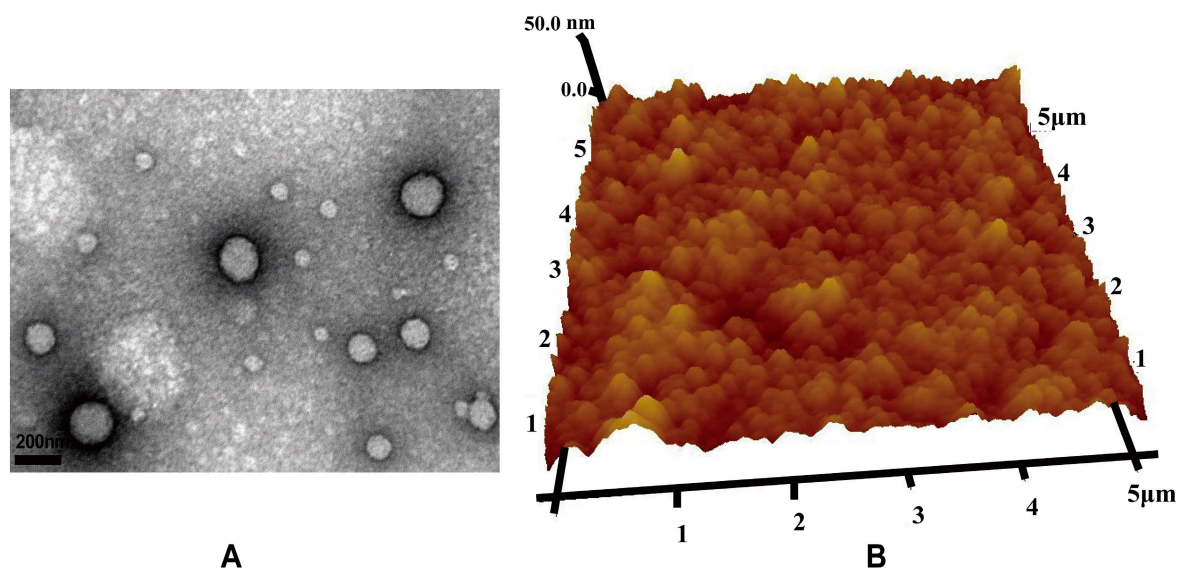

Figure 5. Morphology of VCM/TMC nanoparticles. (**A**) TEM image; and (**B**) AFM image.

All antibiotic-loaded formulations showed good loading efficiency (73.65% $\pm$ 1.83%), while the extent of drug loading, expressed as mass of VCM per mass of nanoparticles, was much lower (5.80% $\pm$ 0.17%). The predominant influencing factor could be the narrow size distribution of the prepared nanoparticles. The nanoparticles were fairly stable for at least two days in Hepes (pH 7.4), with an average SD of 4.41 nm in size (Figure 6).

3.3. In Vitro Drug Release and Kinetic Modeling

The cumulative percentage of drug release was plotted against time to obtain the drug release profile. Figure 7 shows the release behavior of VCM from VCM/TMC nanoparticles over 30 days in PBS (pH 7.4). Accumulative release of the antibiotic followed a steady, continued-release pattern, without a burst release phenomenon, and the time for 50 and 80 wt % release was close to day 14 and day 32

respectively, which satisfied the need for prolonged administration of antibacterial agents after surgical debridement for about 4–6 weeks [14].
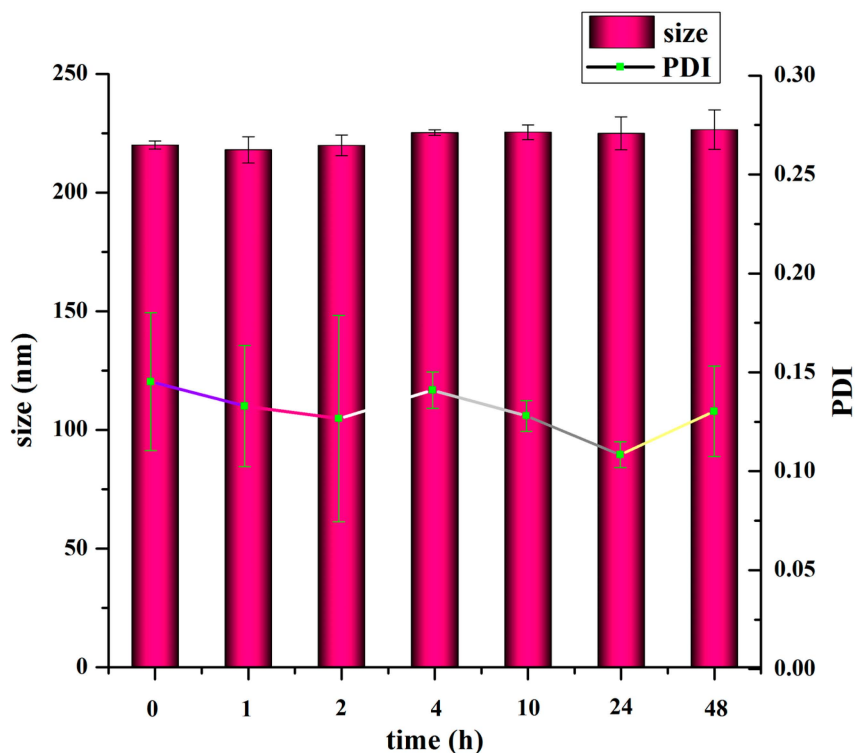

Figure 6. Size and PDI of nanoparticles during 2 days of incubation at 37 °C in Hepes (pH 7.4).
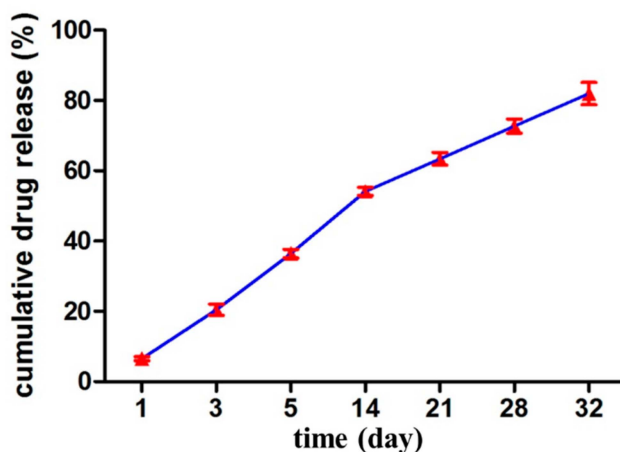

Figure 7. Release of VCM from TMC nanoparticles in PBS (pH 7.4) at 37 °C.

To predict and correlate the release of solutes from nanoparticles *in vitro*, results must be fit into a suitable mathematical model [15,16]. As presented in Figure 8, the data was most suited to the Higuchi model, with a correlation coefficient of 0.9939. According to this model, the liquid penetrates the TMC matrix and dissolves the embedded antibiotics, and so the antibiotic release seems to be a process predominately controlled by diffusion. Similar drug release kinetics were reported for nanoparticles and micelles by Gandhi [15] and Li [16] Based on an "*n*" value (diffusion exponent) between 0.45 and 0.89, obtained from the Korsmeyer–Peppas model, we can conclude that the drug

release was non-Fickian, following an anomalous transport type diffusional release, which exhibited both diffusion- and swelling-controlled drug release. Furthermore, aside from matrix degradation possibly playing a small role, the data are in accordance with that previously described in the Higuchi model.
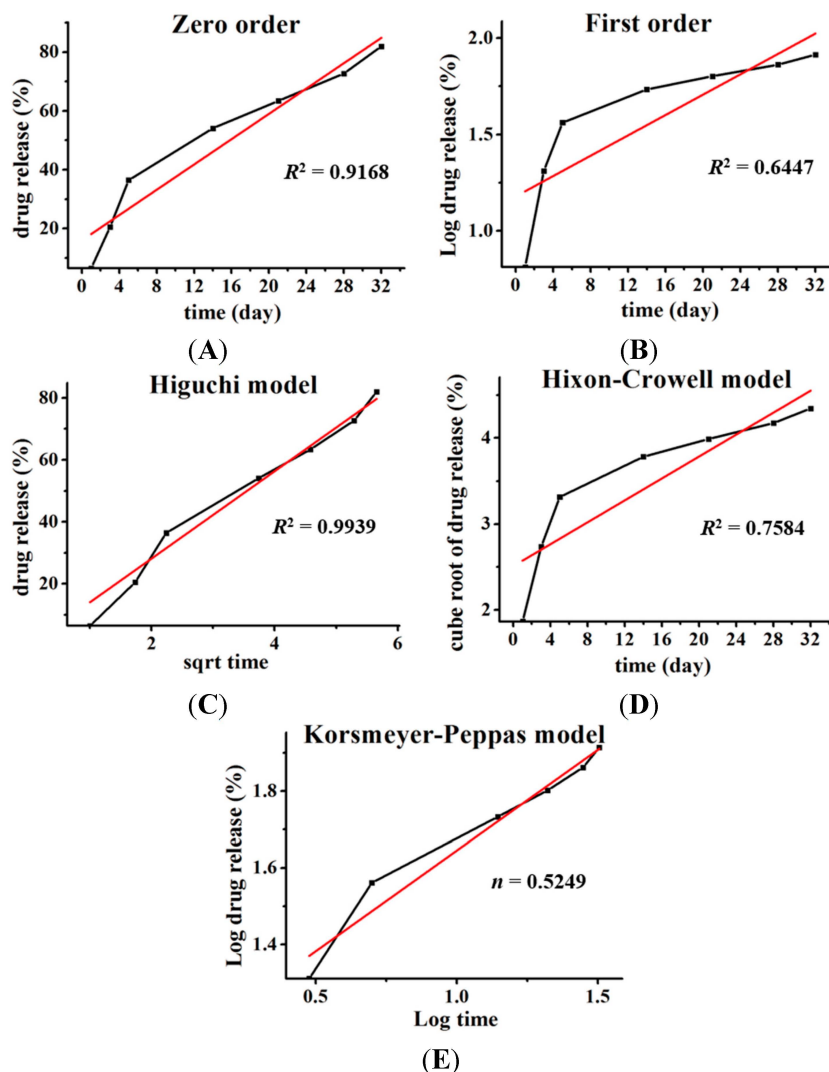

Figure 8. Drug release data fitted to various kinetic models. (**A**) Zero order; (**B**) First order; (**C**) Higuchi model; (**D**) Hixson-Crowell model; and (**E**) Korsmeyer-Peppas drug diffusion model.

3.4. Alkaline Phosphatase Activity

β-TCP has been widely used as a bone substitute material, with the ability to function as a drug delivery vehicle, because of its excellent biocompatibility, osteoconductivity, and osteoinductivity properties [17,18]. We used β-TCP as a control to compare with plain TMC nanoparticles. ALP activity, one of the chief and early biochemical markers of osteoblastic differentiation, can lay the foundation for rapid bone regeneration *in vivo*. Figure 9 shows the ALP activity of β-TCP and the nanoparticle material without antibiotic (TMC-TPP) after day 4 to day 7 of co-incubation with OBs. From day 4 to day 7, no increase in ALP activity was observed ($p > 0.1$) in either the control group or the β-TCP group. On the contrary, cells cultured with TMC-TPP showed a dramatic increase in ALP activity

by nearly 1.5-fold ($p < 0.001$). At day 4, TMC-TPP showed significantly ($p < 0.001$) higher enzyme activity compared with β-TCP and the control. Importantly, after 7 days of incubation, similar results were obtained with significantly ($p < 0.001$) lower ALP vitality in the absence of TMC-TPP. Regarding ALP levels, nanoparticles may therefore be better carriers owing to their positively charged surfaces that allow for better cell adhesion and internalization compared with bioceramic materials, and their enhanced surface area for binding of cells as a result of their spherical nano-structure. These results are in line with Zhang *et al.* [19] and Ko *et al.* [20], who have found that the ALP activity of cultured primary osteoblasts was increased in a time- and dose-dependent manner in the presence of gold nanoparticles (AuNPs) and suggested that the size of nanoparticles maybe the critical factor in regulating osteoblasts activities. Overall, our data clearly demonstrated that the prepared nanoparticles positively accelerated osteoblast differentiation with higher ALP activity.
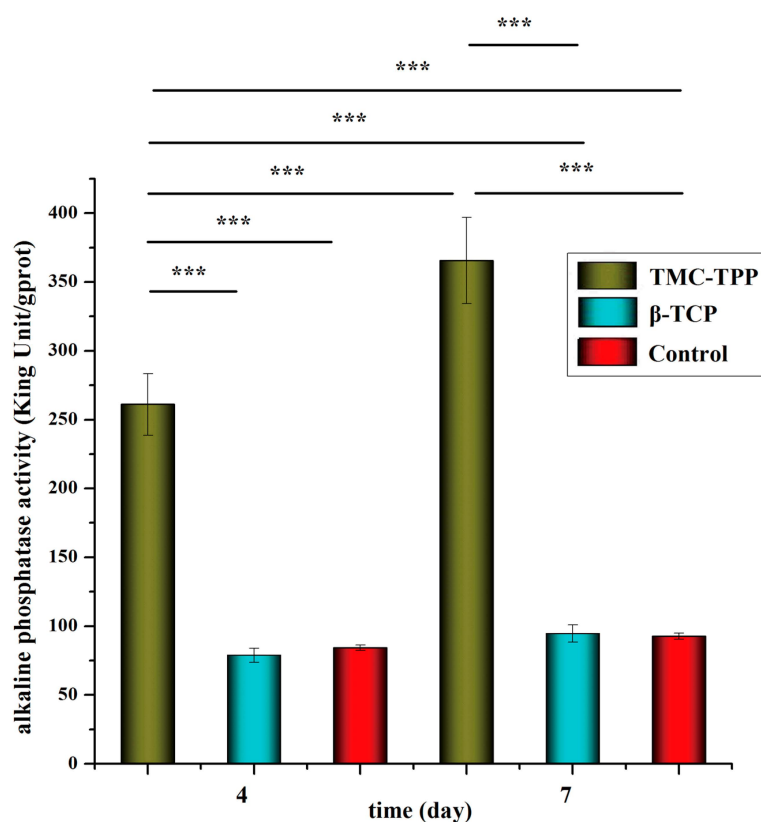

Figure 9. ALP activity of OBs exposed to TMC-TPP nanoparticles and β-TCP suspension. *******, $p < 0.001$.

3.5. Cell Uptake Study

Because the internalization of a drug carrier is crucial to its success as a targeted delivery system, *ex vivo* drug uptake studies of the developed formulations were performed in cultured OB. For that, OBs were stimulated for 4 h with either QDs alone or QDs/TMC-TPPnanocomplexes to investigate if encapsulation of QDs increased their association with OBs. The positively charged QDs/TMC-TPP formulations showed significantly higher cellular uptake ($p < 0.01$) (Figure 10), whereas QDs incorporated in PBS (pH 7.4) were less efficiently taken up by OBs. It is likely that hydrophilic materials block penetration of the hydrophobic cell membrane, and the intracellular penetration of

the nanoparticles mainly depends upon their surface charge and size distribution. Positively charged nanocarriers are better able to facilitate the movement of antibiotics across the OB membrane. These results indicate that TMC nanoparticles can improve delivery of water-soluble antibiotics across cytomembrane barriers to infection sites that are almost inaccessible to conventional treatments.
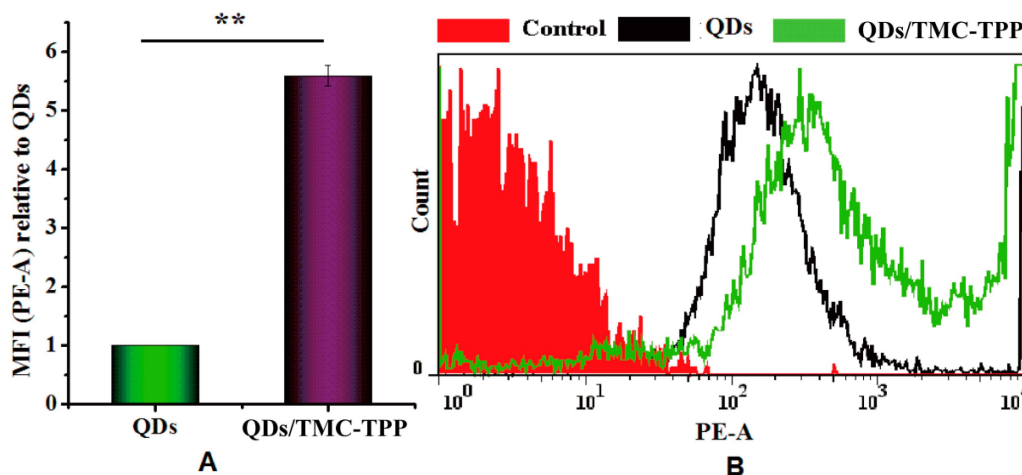

Figure 10. *In vitro* cell uptake by osteoblasts (OBs). OBs were exposed to soluble or nanoparticle-encapsulated QDs for 4 h and measured by flow cytometry. (**A**) Uptake expressed by mean fluorescence intensity and (**B**) Data expressed by representative overlay histogram. ******, $p < 0.01$.

3.6. Cell Proliferation

The *in vitro* proliferation activity of VCM/TMC nanoparticles was compared with that of other VCM formulations by MTT assay. Although the MTT assay cannot accurately determine exact numbers of cells, it measures cell metabolic activity, which is proportional to cell numbers under similar culture conditions. Figure 11 shows the cell viability of test subjects. After co-cultivation for 48 h, VCM-loaded TMC nanoparticles elicited significantly higher cell proliferation (approximately 2.5 times, $p < 0.001$) activity compared with VCM solutions having the same antibiotic concentration. Similar results were obtained with significantly ($p < 0.05$) lower toxicity of VCM/TMC solution compared with VCM solution. The MTT experiments also clearly showed that the order of the cell viabilities was VCM/TMC nanoparticle (VCM/TMC-TPP) > VCM/TMC solution (VCM/TMC) > VCM solution (VCM) > control. This proliferative effect was mainly driven by its biocompatibility and nano-structure, which is in agreement with previous studies done by Yeon *et al.* [21] on osteoblast cells that adhesion and proliferation of osteoblasts could be influenced by varying the nano-structured surfaces and fixed the surface structure in the nanometer size scale could be useful for designing novel scaffolds in tissue engineering applications. Besides, since this effect remained slightly present in the VCM solution group, it may be partly ascribed to the intracellular biological environments that were produced by antibiotics with a proper low concentration. Therefore, it is reasonable to conclude that the current prepared VCM/TMC nanoparticles are not only cytocompatible but also significantly stimulate the proliferation of OBs, which is fundamental to induce bone regeneration.
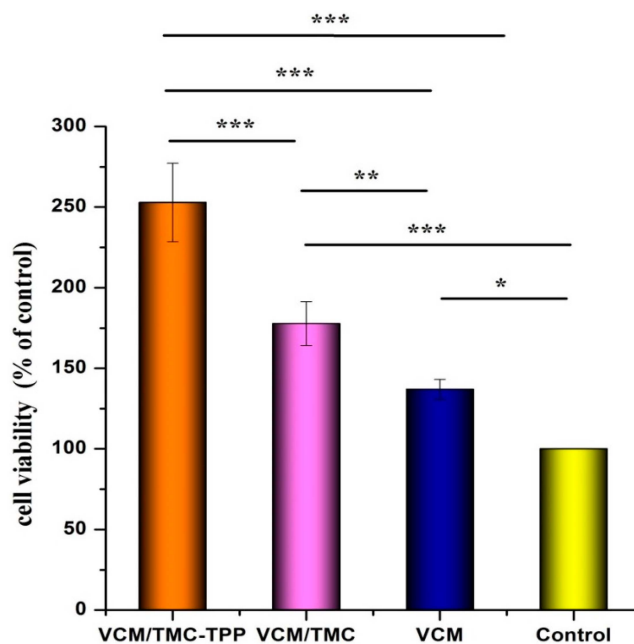
Figure 11. MTT (3-(4,5-dimethylthiazol-2-yl)-2,5-diphenyltetrazolium bromide) assay for cell proliferation activity *in vitro*. ***, $p < 0.001$; **, $p < 0.01$; and *, $p < 0.05$.

3.7. The Antibacterial Activities

We performed MIC and IC50 tests on *S. aureus* to preliminarily investigate the antibacterial activity of VCM/TMC nanoparticles (VCM/TMC-TPP). As shown in Table 1, the MIC value of VCM solutions was estimated to be 80 μg/mL, however, the value toward VCM/TMC nanoparticles was much lower at about 60 μg/mL. A lower MIC value corresponds to higher antibacterial effectivenesss [22]. Thus, it is reasonable to expect that the nanoparticles prepared in this study have an increased bacteriostatic effect compared with the solution alone. In addition, the IC50 values of VCM/TMC nanoparticles and VCM solutions against the growth of *S. aureus* for 24 h were 48.47 and 64.81 μg/mL, respectively (Figure 12), which are consistent with the results of the MIC test.

Table 1. Minimum inhibitory concentration (MIC) test of various concentrations of vancomycin/*N*-trimethyl chitosan (VCM/TMC) nanoparticle and VCM solution against *S. aureus*. "+" for bacterial growth, "−"for no bacterial growth.

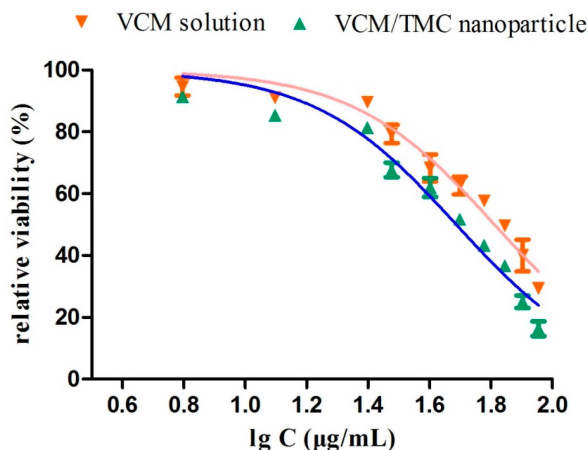| Concentrations (μg/mL)	VCM/TMC-TPP	VCM
6.25	+	+
12.5	+	+
25	+	+
50	+	+
60	−	+
70	−	+
80	−	−
90	−	−

Figure 12. IC50 test of various concentrations of VCM/TMC nanoparticles and VCM solution against *S. aureus*.

Furthermore, a growth inhibition assay was used to investigate the susceptibility of *S. aureus* to VCM/TMC nanoparticles. Compared with the VCM solution group treated with concentrations of 50, 60, 70 and 80 μg/mL, there was an obviously visible DIZ around VCM/TMC nanoparticle-coated paper discs and the values were 0.805, 0.905, 0.905 and 1.050 cm, respectively (Figure 13B), but 0.750, 0.755, 0.805 and 0.805 cm, respectively, for VCM solutions (Figure 13A). Finally, the antibacterial activity of VCM/TMC nanoparticles was further confirmed using the TB assay. As presented in Figure 14, with increasing concentration of VCM in both the VCM/TMC nanoparticles and VCM solutions, ranging from 6.25 to 90 μg/mL, the percentage bacteria viability decreased. Notably, at 70 μg/mL VCM, nanoparticles were significantly more effective at slowing the growth of *S. aureus* ($p < 0.001$). Furthermore, approximately 30% of *S. aureus* survived when the concentration of VCM/TMC nanoparticles was raised to 70 μg/mL, whereas it was 90 μg/mL for the solution group.
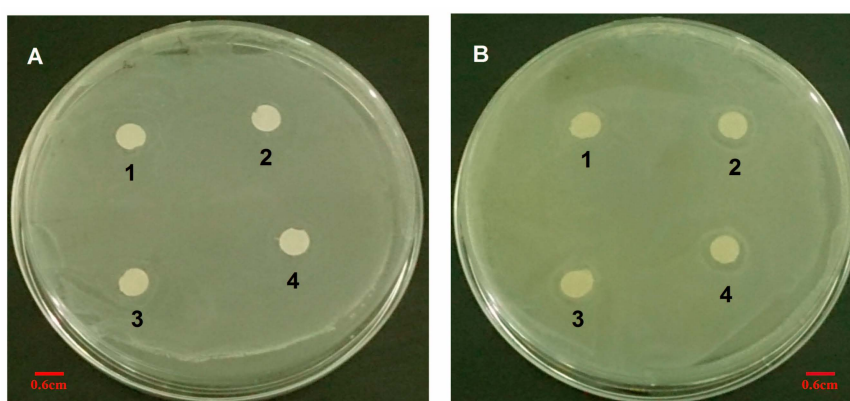

Figure 13. Diameter of inhibition zone test of (**A**) VCM solution and (**B**) VCM/TMC nanoparticles against *S. aureus*. (1). 50 μg/mL; (2). 60 μg/mL; (3). 70 μg/mL; and (4). 80 μg/mL in the LB agar dishes.
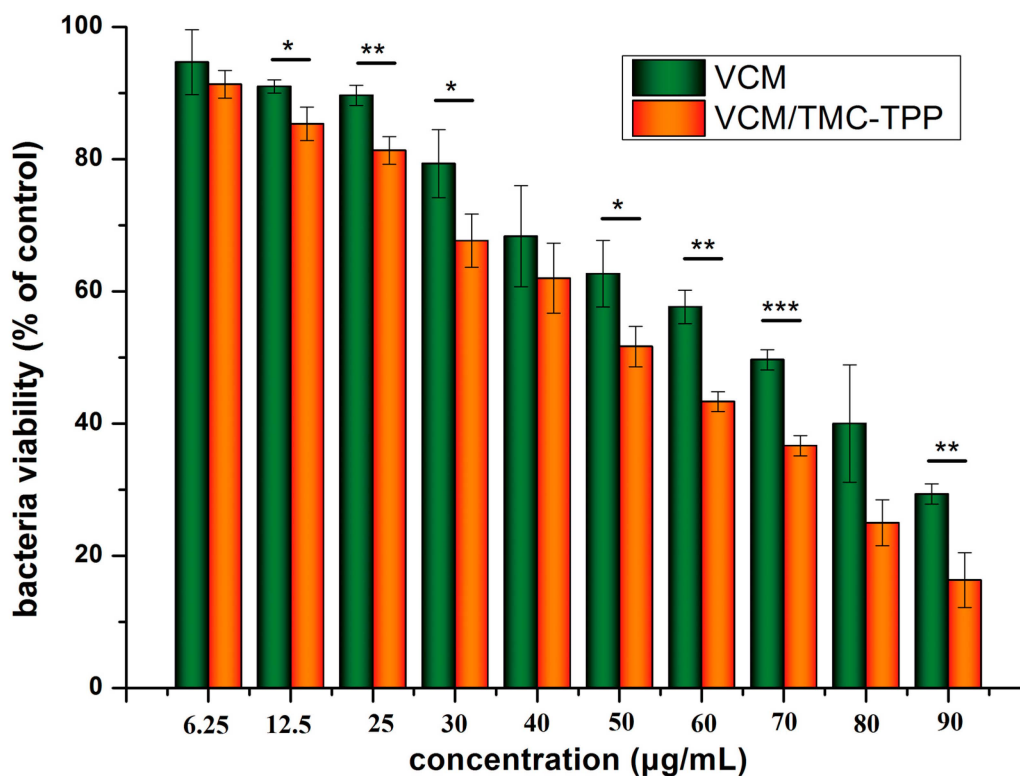
Figure 14. TB assay of VCM/TMC nanoparticles and VCM solution against *S. aureus*. ***, $p < 0.001$; **, $p < 0.01$; and *, $p < 0.05$.

4. Conclusions

This work has demonstrated that rationally designed antibiotic VCM-loaded TMC nanoparticles can be readily prepared using ionic complexation, with high drug loading capacity and steady, continued release. After treatment with TMC-TPP, OBs exhibit high ALP activity. The nanoparticles were efficiently taken up into OBs, showing that they can be useful nanocarriers for the intracellular delivery of various antibiotics. OBs exposed to VCM/TMC nanoparticles exhibited very high cell proliferative ability, more easily establishing a desired cell population. Furthermore, the results of MIC, IC50, DIZ and TB assays, all indicate the excellent antibacterial activity of VCM/TMC nanoparticles against the Gram-positive *S. aureus*, thus making it a novel antibacterial candidate substance for the treatment of bacterial infections. In summary, the VCM/TMC nanoparticles are effective intracellular drug carriers owing to their positively charged surface, suitable size distribution, sustained release profiles, good cell uptake activity, ability to induce OB proliferation and excellent antibacterial activity. These nanoparticles thus can be a promising strategy to treat intracellular infections such as chronic osteomyelitis.

In addition, our further work is currently in progress to use poly-(trimethylene carbonate) (PTMC), a kind of surface-eroding biodegradable material [23], which is fully biocompatible [24], and exhibits an ideal sustained, zero order release profile and also promotes bone regeneration [25], to prepare VCM/TMC nanoparticle-loaded PTMC local drug delivery system, with a view to treating chronic osteomyelitis that is caused by intracellular infections in human patients.

Acknowledgments

Author Contributions

Ying Hu was mainly engaged in the research design; the main parts of the research experiments were done by JiaoJiao Xu and Beihua Xu; Dan Shou and Xiaojing Xia were writers and validators of the paper.

Conflicts of Interest

The authors declare no conflict of interest.

References

1. Abed, N.; Couvreur, P. Nanocarriers for antibiotics: A promising solution to treat intracellular bacterial infections. *Int. J. Antimicrob. Agents* **2014**, *43*, 485–496. [CrossRef] [PubMed]

2. Xiong, M.H.; Bao, Y.; Yang, X.Z.; Zhu, Y.H.; Wang, J. Delivery of antibiotics with polymeric particles. *Adv. Drug Deliv. Rev.* **2014**, *78*, 63–76. [CrossRef] [PubMed]

3. Costerton, J.W.; Lewandowski, Z.; Caldwell, D.E.; Korber, D.R.; Lappin-Scott, H.M. Microbial biofilms. *Annu. Rev. Microbiol.* **1995**, *49*, 711–745. [CrossRef] [PubMed]

4. Uskokovic, V.; Desai, T.A. Simultaneous bactericidal and osteogenic effect of nanoparticulate calcium phosphate powders loaded with clindamycin on osteoblasts infected with staphylococcus aureus. *Mater. Sci. Eng. C* **2014**, *37*, 210–222. [CrossRef] [PubMed]

5. Huh, A.J.; Kwon, Y.J. "Nanoantibiotics": A new paradigm for treating infectious diseases using nanomaterials in the antibiotics resistant era. *J. Control. Release* **2011**, *156*, 128–145. [CrossRef] [PubMed]

6. Zakeri-Milani, P.; Loveymi, B.D.; Jelvehgari, M.; Valizadeh, H. The characteristics and improved intestinal permeability of vancomycin PLGA-nanoparticles as colloidal drug delivery system. *Colloids Surf. B* **2013**, *103*, 174–181. [CrossRef] [PubMed]

7. Kalhapure, R.S.; Mocktar, C.; Sikwal, D.R.; Sonawane, S.J.; Kathiravan, M.K.; Skelton, A.; Govender, T. Ion pairing with linoleic acid simultaneously enhances encapsulation efficiency and antibacterial activity of vancomycin in solid lipid nanoparticles. *Colloids Surf. B* **2014**, *117*, 303–311. [CrossRef] [PubMed]

8. Sindhura Reddy, N.; Sowmya, S.; Bumgardner, J.D.; Chennazhi, K.P.; Biswas, R.; Jayakumar, R. Tetracycline nanoparticles loaded calcium sulfate composite beads for periodontal management. *Biochim. Biophys. Acta Gen. Subj.* **2014**, *1840*, 2080–2090. [CrossRef] [PubMed]

9. Mansur, H.S.; Mansur, A.A.; Curti, E.; de Almeida, M.V. Bioconjugation of quantum-dots with chitosan and *N,N,N*-trimethyl chitosan. *Carbohydr. Polym.* **2012**, *90*, 189–196. [CrossRef] [PubMed]

10. De Britto, D.; Celi Goy, R.; Campana Filho, S.P.; Assis, O.B.G. Quaternary salts of chitosan: History, antimicrobial features, and prospects. *Int. J. Carbohydr. Chem.* **2011**, *2011*, 12. [CrossRef]

11. Amidi, M.; Romeijn, S.G.; Borchard, G.; Junginger, H.E.; Hennink, W.E.; Jiskoot, W. Preparation and characterization of protein-loaded *N*-trimethyl chitosan nanoparticles as nasal delivery system. *J. Control. Release* **2006**, *111*, 107–116. [CrossRef] [PubMed]

12. Verheul, R.J.; Amidi, M.; van der Wal, S.; van Riet, E.; Jiskoot, W.; Hennink, W.E. Synthesis, characterization and *in vitro* biological properties of *O*-methyl free *N,N,N*-trimethylated chitosan. *Biomaterials* **2008**, *29*, 3642–3649. [CrossRef] [PubMed]

13. Bal, S.M.; Slutter, B.; van Riet, E.; Kruithof, A.C.; Ding, Z.; Kersten, G.F.; Jiskoot, W.; Bouwstra, J.A. Efficient induction of immune responses through intradermal vaccination with *N*-trimethyl chitosan containing antigen formulations. *J. Control. Release* **2010**, *142*, 374–383. [CrossRef] [PubMed]

14. Rao, N.; Lipsky, B.A. Optimising antimicrobial therapy in diabetic foot infections. *Drugs* **2007**, *67*, 195–214. [CrossRef] [PubMed]

15. Gandhi, A.; Jana, S.; Sen, K.K. *In-vitro* release of acyclovir loaded Eudragit RLPO® nanoparticles for sustained drug delivery. *Int. J. Biol. Macromol.* **2014**, *67*, 478–482. [CrossRef] [PubMed]

16. Li, W.; Peng, H.; Ning, F.; Yao, L.; Luo, M.; Zhao, Q.; Zhu, X.; Xiong, H. Amphiphilic chitosan derivative-based core-shell micelles: Synthesis, characterisation and properties for sustained release of vitamin D$_3$. *Food Chem.* **2014**, *152*, 307–315. [CrossRef] [PubMed]

17. Nandi, S.K.; Ghosh, S.K.; Kundu, B.; de, D.K.; Basu, D. Evaluation of new porous β-tri-calcium phosphate ceramic as bone substitute in goat model. *Small Rumin. Res.* **2008**, *75*, 144–153. [CrossRef]

18. Nandi, S.K.; Mukherjee, P.; Roy, S.; Kundu, B.; de, D.K.; Basu, D. Local antibiotic delivery systems for the treatment of osteomyelitis—A review. *Mater. Sci. Eng. C* **2009**, *29*, 2478–2485. [CrossRef]

19. Zhang, D.; Liu, D.; Zhang, J.; Fong, C.; Yang, M. Gold nanoparticles stimulate differentiation and mineralization of primary osteoblasts through the ERK/MAPK signaling pathway. *Mater. Sci. Eng. C* **2014**, *42*, 70–77. [CrossRef] [PubMed]

20. Ko, W.K.; Heo, D.N.; Moon, H.J.; Lee, S.J.; Bae, M.S.; Lee, J.B.; Sun, I.C.; Jeon, H.B.; Park, H.K.; Kwon, I.K. The effect of gold nanoparticle size on osteogenic differentiation of adipose-derived stem cells. *J. Colloid Interface Sci.* **2015**, *438*, 68–76. [CrossRef] [PubMed]

21. Yeon, S.J.; Lee, J.W.; Lee, J.W.; Kwark, Y.J.; Kim, S.H.; Lee, K.Y. Effect of nano-structured polymer surfaces on osteoblast adhesion and proliferation. *J. Control. Release* **2011**, *152*, e257–e258. [CrossRef] [PubMed]

22. Prucek, R.; Tucek, J.; Kilianova, M.; Panacek, A.; Kvitek, L.; Filip, J.; Kolar, M.; Tomankova, K.; Zboril, R. The targeted antibacterial and antifungal properties of magnetic nanocomposite of iron oxide and silver nanoparticles. *Biomaterials* **2011**, *32*, 4704–4713. [CrossRef] [PubMed]

23. Bat, E.; van Kooten, T.G.; Feijen, J.; Grijpma, D.W. Macrophage-mediated erosion of gamma irradiated poly(trimethylene carbonate) films. *Biomaterials* **2009**, *30*, 3652–3661. [CrossRef] [PubMed]

24. Zhang, Z.; Kuijer, R.; Bulstra, S.K.; Grijpma, D.W.; Feijen, J. The *in vivo* and *in vitro* degradation behavior of poly(trimethylene carbonate). *Biomaterials* **2006**, *27*, 1741–1748. [CrossRef] [PubMed]

25. Van Leeuwen, A.C.; van Kooten, T.G.; Grijpma, D.W.; Bos, R.R. *In vivo* behaviour of a biodegradable poly(trimethylene carbonate) barrier membrane: A histological study in rats. *J. Mater. Sci.* **2012**, *23*, 1951–1959. [CrossRef] [PubMed]